FRANK I. GONZALEZ, BENJAMIN M. HOLT, and DAVID G. TILLEY

THE AGE AND SOURCE OF OCEAN SWELL OBSERVED IN HURRICANE JOSEPHINE

The SIR-B mission has yielded exceptionally valuable swell observations in the far field of Hurricane Josephine. This article applies a very simple kinematic model to provide estimates of the swell origin in space and time.

INTRODUCTION

The unfortunate mariner caught in a hurricane experiences only a limited portion of its awesome size and force. A severely limited vantage point and understandable preoccupation with survival make large-scale structure and order difficult to perceive. Chaos seems to reign.

However, in-situ instrumentation fortuitously placed in the path of a cyclone can provide more objective and systematic observations that, when suitably averaged, reveal smooth temporal variations of properties such as wind velocity and significant wave height. If steady state is assumed, these temporal variations can be interpreted in terms of spatial gradients swept through the observation point at constant velocity—a straightforward application of what is known as Taylor's hypothesis. The results suggest order and organization in hurricanes over such large areas that the need for larger scale observations becomes apparent.

In meteorological research, routine aircraft observations have helped fill the need for large-scale observations. More recently, operational weather satellites have provided meteorologists with frequent snapshots of entire cyclonic systems. Each step back to a more comprehensive vantage point for viewing large-scale structure has greatly enhanced the value of in-situ measurements by providing a better context for interpretation. This has led to a better understanding of the fundamental physical processes governing hurricane genesis and evolution, with concommitant improvements in operational forecasting.[1-5]

In contrast, research on ocean-wave generation and propagation currently suffers from a lack of comparable observations of large-scale patterns of directional energy spectra produced by hurricanes and other meteorological systems. In the last 70 years, investigators have progressed from visual reports to in-situ and airborne instrumentation and, in the last decade, to observations from spacecraft, using remote-sensing techniques.[6-15] However, these measurements of directional spectra are still in the experimental stage and are not made on a routine operational basis.

Early attempts to discern large-scale patterns of wave energy distribution in hurricanes applied Taylor's hypothesis to visual estimates acquired along a coast or by ships at sea.[6,7] In the decades that followed, technological advances provided objective in-situ wave-measurement capabilities that have been extremely valuable in guiding hurricane wave research.[8-10] However, the vast majority of ocean-wave field data consists of simple time series of sea level at a single point; such data yield estimates of wave energy as a function of frequency but fail to provide critically important information on the directional distribution of this energy. Pitch–roll–heave buoys can provide such directional estimates, and the National Oceanic and Atmospheric Administration (NOAA) has deployed and tested prototype directional buoys that will eventually be incorporated into the operational network maintained by the NOAA Data Buoy Center (NDBC).[11] The routine collection of such information will be extremely valuable; however, the directional resolution of the in-situ system is quite coarse, and the data are still limited to a single point. Furthermore, the data network will be very sparse; currently, logistics problems restrict buoy sites to a region less than a thousand kilometers from the coast, and the relatively small number of buoys deployed results in spacing on the order of hundreds of kilometers. Even if Taylor's hypothesis is invoked, such data can only hint at the large-scale patterns of directional wave energy spectra induced by hurricanes.

Aircraft observations can help fill the need for wave measurements over large spatial scales. Unfortunately, an operational program for the routine acquisition of

Frank I. Gonzalez is a physical oceanographer at the NOAA Pacific Marine Environmental Laboratory, Seattle, WA 98115.

Benjamin M. Holt is a research scientist in the Earth and Space Sciences Division, NASA/Jet Propulsion Laboratory, Pasadena, CA 91109. David G. Tilley is a senior staff engineer in the Space Geophysics Group, The Johns Hopkins University Applied Physics Laboratory, Laurel, MD 20707.

hurricane wave data by aircraft does not exist; consequently, the existing database collected in this way is relatively small. Of particular interest are those few observations that have provided directional wave information over relatively large oceanic regions by means of imaging or altimetric radar systems.[12-14]

Spaceborne remote-sensing instruments promise even more comprehensive views of ocean-wave patterns in the near- and far-field of hurricanes and other meteorological systems; before the untimely failure of Seasat, the synthetic aperture radar on board provided directional wave information for at least two hurricane studies.[15,16] However, those studies were handicapped by the relatively high Seasat orbit of 800 kilometers; the resulting geometry was less than optimal for imaging ocean waves, and wavenumber vector estimates were consequently degraded by significant azimuthal smearing, especially in regions of high sea state. This source of error can be greatly reduced by lower spacecraft orbits, as was demonstrated by the recent SIR-B mission, flown at a height of 230 kilometers.[17] Furthermore, recent improvements in modeling the ocean-wave/synthetic aperture radar transfer function promises to add energy estimates to those of wavelength and direction, thus greatly increasing the value of such data (see the articles by Lyzenga and by Monaldo elsewhere in this issue).

This article provides a preliminary analysis of a limited portion of the latest hurricane wave data to be acquired from space—the synthetic aperture radar observations of Josephine obtained by the SIR-B mission of the space shuttle Challenger. The basic philosophy guiding this work is that the beautiful and strikingly smooth swell patterns seen in the SIR-B imagery can be meaningfully interpreted in terms of simple wave kinematics and idealized hurricane geometry and, furthermore, that such an approach can provide new insights into the physical mechanisms governing the generation and propagation of waves in real hurricanes.

DATA

Josephine began to develop on October 7, 1984, as a very large and diffuse subtropical low east of the central Bahamas; it began to drift west, then west-northwest on October 8. She became not only the largest cyclone of the season, but also the longest lived. Evidently, the combination of a cool oceanic environment and unusual system size resulted in a very slow strengthening process. Traveling due north at a speed of 4 to 5 meters per second, Josephine slowly intensified for a full two days before finally attaining hurricane strength on October 10. She slowly continued to strengthen for another two days before maximum sustained winds of 90 knots were recorded at 0000 GMT on October 12; these maximum winds evidently persisted for at least 18 hours (until 1800 GMT).[18]

Sixteen and one-half hours after Josephine reached maximum intensity, the space shuttle Challenger, on orbit 117 of the SIR-B mission, acquired one and one-half minutes of SAR imagery near Josephine.[19] The resulting image swath was over 650 kilometers long and 25 kilometers wide; it lay north and east of the hurricane position at a 45 degree angle to the storm track and came within 90 kilometers of the hurricane center at its closest point (Fig. 1).

Digitally processed imagery, subsampled to a square pixel size of 12.5 meters, was provided by the Jet Propulsion Laboratory. Two strips of imagery were selected along the near and far edge of the image swath. Each strip was then partitioned into 100 approximately contiguous square segments, 512 pixels (or 6.4 kilometers) on a side. After subtraction of the mean intensity value, a circular cosine taper was applied; each subimage was then subjected to Fourier transformation to provide two-dimensional image intensity spectra. After application of a correction for the SIR-B stationary response function, the results were scaled and smoothed by a 15 × 15 Gaussian filter; consequently, individual spectral estimates of the final products (Fig. 2) are characterized by approximately 300 degrees of freedom. Additional details of this process are presented in the article by Tilley elsewhere in this issue.

ANALYSIS

In this preliminary study, we idealize hurricane swell propagation by the simple conceptual model sketched

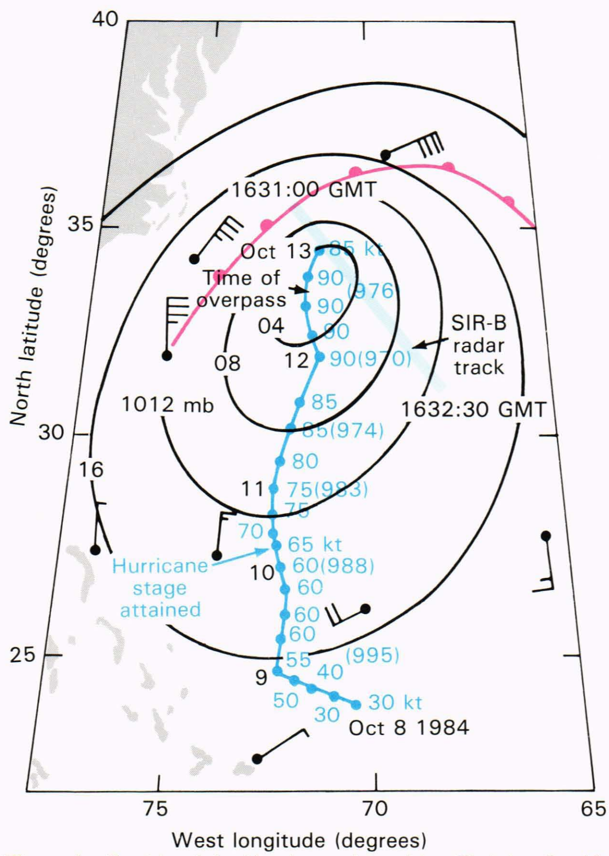

Figure 1—Best track for Hurricane Josephine (October 8 – 13, 1984) and location of SIR-B imagery collected on October 12, 1984. Estimates of Josephine's maximum wind speed in knots are indicated at 6-hour intervals along the track, and sea level pressure is given in parentheses in millibars at selected times. Surface pressure field and wind observations were for 1200 GMT, October 12, 1984.

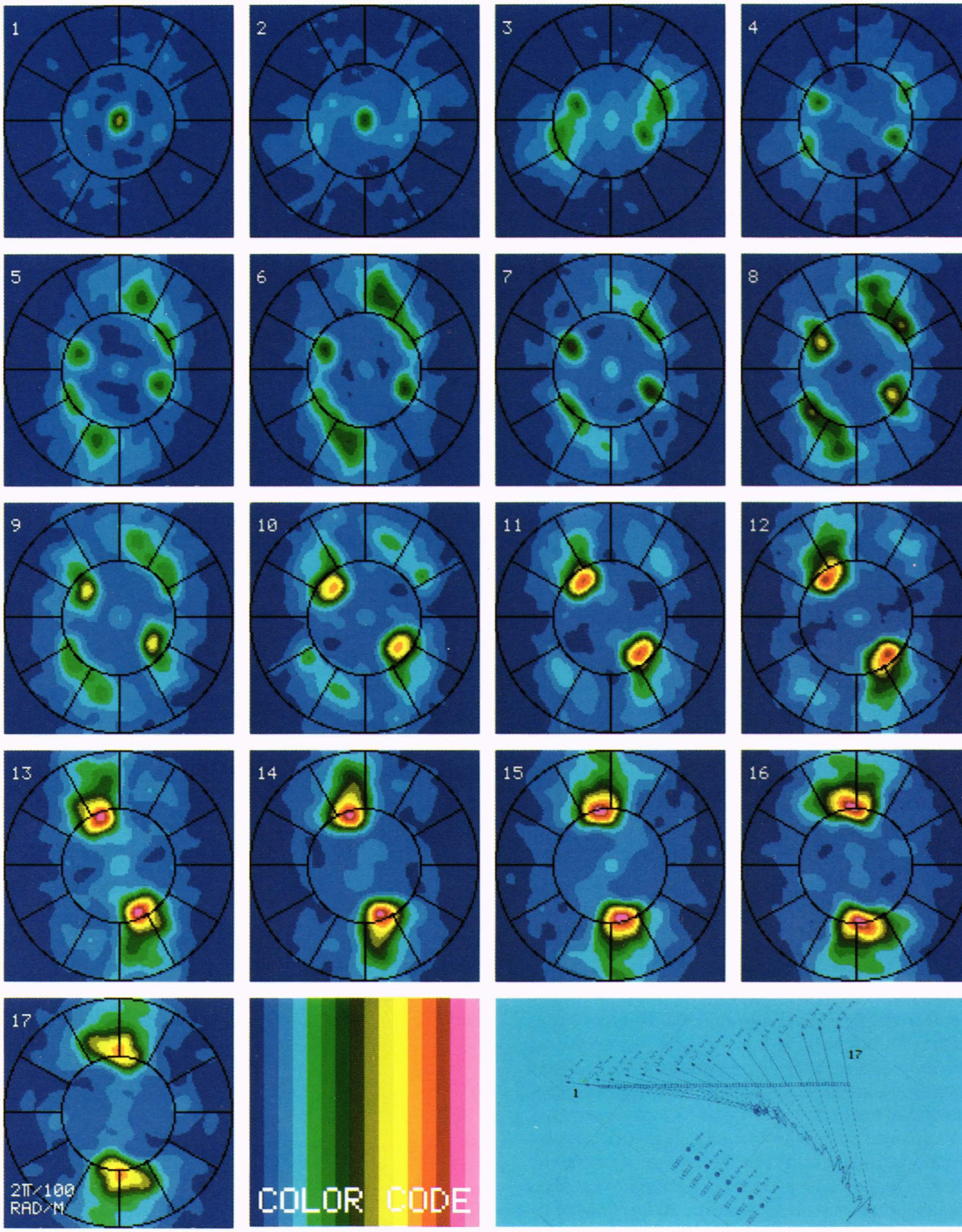

Figure 2—SAR image intensity spectra derived by two-dimensional fast Fourier transform of selected SIR-B subimages. The relative location of each subimage is shown in the inset in the lower right-hand corner. Processing details are discussed in the text.

in Fig. 3. We assume the existence of a unique space-time source point, $S\ (x_s, y_s, t_s)$, that identifies the "birth" of an individual swell system characterized by wavenumber, κ, and direction, θ. Swell birth is defined

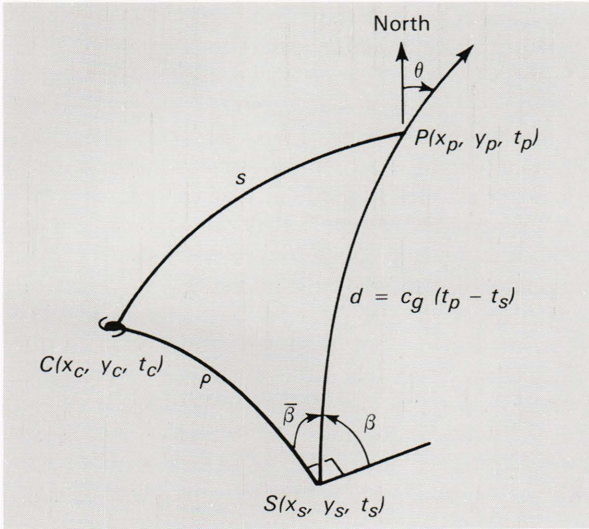

Figure 3—Geometry of the idealized hurricane swell kinematic model. The point C represents the center of the hurricane, P is a point at which a dominant wavenumber vector is observed, and S is the point of origin of the swell.

as that point when the deep-water group speed,

$$c_g = (gk)^{1/2}, \quad (1)$$

exceeds the local wind-speed component in the wave direction. The wave then ceases to be forced by the wind and begins to propagate freely as swell. This can occur if local wind speed decreases, if forced waves move into regions of lower winds, or both. Similarly, swell can "die" and revert to forced waves if the local wind increases, if swell propagates into sufficiently higher wind regions, or both. Eventually, however, perhaps after multiple reincarnations, swell systems escape the influence of high winds in the hurricane near field and propagate into the far field, characterized by relatively lower wind speeds.

We now make an important simplifying assumption, namely, that such swell consists of truly free waves and is unaffected by processes such as wave–wave interaction and refraction by surface currents. Thus, if swell is born at the space–time source point $S(x_s,y_s,t_s)$, propagation proceeds along a great-circle route for time $dt = (t_p - t_s)$ to the observation point $P(x_p,y_p,t_p)$. Spherical geometry (Fig. 3) then determines the following relationships:

$$\beta = 90 - \cos^{-1}\left[\frac{\cos s - \cos d \cos \rho}{\sin d \sin \rho}\right], \quad (2a)$$

$$s = \cos^{-1}[\cos \bar{y}_c \cos \bar{y}_p + \sin \bar{y}_c \sin \bar{y}_p \times \cos (x_p - x_c)] , \quad (2b)$$

$$\rho = \cos^{-1}[\cos \bar{y}_c \cos \bar{y}_s + \sin \bar{y}_c \sin \bar{y}_s \times \cos (x_s - x_c)] , \quad (2c)$$

$$x_s = x_p + \cos^{-1}\left[\frac{\cos d - \cos \bar{y}_p \cos \bar{y}_s}{\sin \bar{y}_p \sin \bar{y}_s}\right], \quad (2d)$$

$$\bar{y}_s = \cos^{-1}[\cos d \cos \bar{y}_p + \sin d \sin \bar{y}_p \times \cos (180 - \theta)] , \quad (2e)$$

and

$$d = c_g \, \Delta t = ½ \, (gk)^{1/2} \, (t_p - t_s) , \quad (2f)$$

where overbars denote co-angles, i.e.,

$$\bar{y} = 90 - y .$$

In these relationships, if the quantities

$[x_c(t), y_c(t)]$	=	hurricane center longitude and latitude, respectively, at time t
(x_p, y_p, t_p)	=	observation point, P
(κ_p, θ_p)	=	wavenumber vector at observation point P
$\beta(t)$	=	the wave inflow angle at time t

are assumed known, then Eq. 2 is a system of equations for the unknown age of the swell, dt, and the associated source longitude and latitude, (x_s, y_s).

Hurricane center fixes are acquired by the NOAA National Hurricane Center in Miami, Florida, from aerial reconnaissance penetrations, satellite imagery, and land-based radar.[20] These raw hurricane position data are then examined by experienced hurricane specialists at a later date, when there is more time to examine important additional information not available earlier, such as additional ship reports and the final versions of surface and upper level pressure analyses. This process results in a smoother estimate of successive hurricane positions that are known as "best tracks."

In order to provide continuous expressions for our numerical computation, we performed least-square fits of polynomials to the best-track latitudes and longitudes as a function of time. The resulting polynomials provide positions that reproduce the best track values to within 5 kilometers. Since this level of accuracy is generally considered to be equal to or better than the best-track estimates themselves, the least-square fit polynomials were adopted in this work as the required hurricane center longitude and latitude functions, $x_c(t), y_c(t)$.

The coordinates (x_p, y_p, t_p) for each observation point were computed using location algorithms provided by the Jet Propulsion Laboratory. These algorithms estimate geodetic coordinates for a given pixel in the geometrically corrected imagery and are considered accurate to about 300 meters for SIR-B data.[21] Each point corresponds to the center pixel of a scene subjected to fast Fourier transformation.

The dominant wavenumber and angle (κ, θ) for the system studied here were estimated by identifying local maxima in the fast Fourier transform, locating the closed contour representing 95 percent of the maximum value, and then computing the center of mass of this subregion. Only one dominant wave system in 100 of the spectra has been analyzed so far, corresponding to the image strip farthest from the hurricane track. The results for 20 of the spectra are plotted in Fig. 4. Beal et al.[17] and Monaldo and Lyzenga (elsewhere in this issue) find strong evidence that SIR-B image intensity spectra are more closely related to ocean-wave slope spectra rather than height spectra. However, it was also found that while the shapes of the slope spectra and the height spectra differed, in the higher sea states the location of maxima were approximately the same and agreed well with independent observations of dominant ocean wavelength and direction (see the article by Beal elsewhere in this issue).

The angle β is the ocean-swell direction referred to the tangent of a circle of radius ρ centered on the hurricane position. The range of β must be similar to the range of the hurricane wind inflow angle, which is generally observed to vary from 0 degrees near the center to about 20 degrees in the far field. In this study we solved system 2 for the two constant values of $\beta = 0$ and $\beta = 20$ degrees.

RESULTS AND DISCUSSION

The results are presented in Figs. 4a and 4b; the map projections are gnomic, so that great-circle paths are straight lines. Every fifth wavenumber vector is plotted, and the corresponding age estimate is provided near the arrowhead. The age corresponds to the solution, dt, of system 2 and represents the difference between the time of SIR-B data acquisition (approximately 1631:00 to 1632:30 GMT) and the time of generation. The dotted lines are great-circle paths of length d appropriate to the wave age and group velocity, and the open circles represent the points at which, in this simple kinematic model, the wave escaped the influence of wind forcing and began to travel as free swell. Between each circle there are four intermediate points connected by straight lines; these points correspond to the intervening wavenumber estimates for which no vector has been plotted. If a line were to be drawn from these generation points to the storm track position that matches the age of the wave, the angle co-β so formed would be 90 degrees in Fig. 4a ($\beta = 0$) and 70 degrees in Fig. 4b ($\beta = 20$). Storm track positions are indicated by solid dots, marked with Greenwich Mean Time (Z) to the left and estimated wave age to the right.

This extremely simple analysis provides some very interesting qualitative information on the wave system examined. Referring to Fig. 4, the oldest waves were generated only 7 to 9 hours before the SIR-B overpass, and these are found at each end of the 600-kilometer strip of imagery. The wave age decreases and reaches a minimum about midway along the strip, and these waves are apparently 0 to 3 hours old; i.e., they were generated by Josephine between 1330 and 1630 GMT, at a distance of about 200 kilometers from the center and at an azimuth of 80 to 110 degrees with respect to the direction

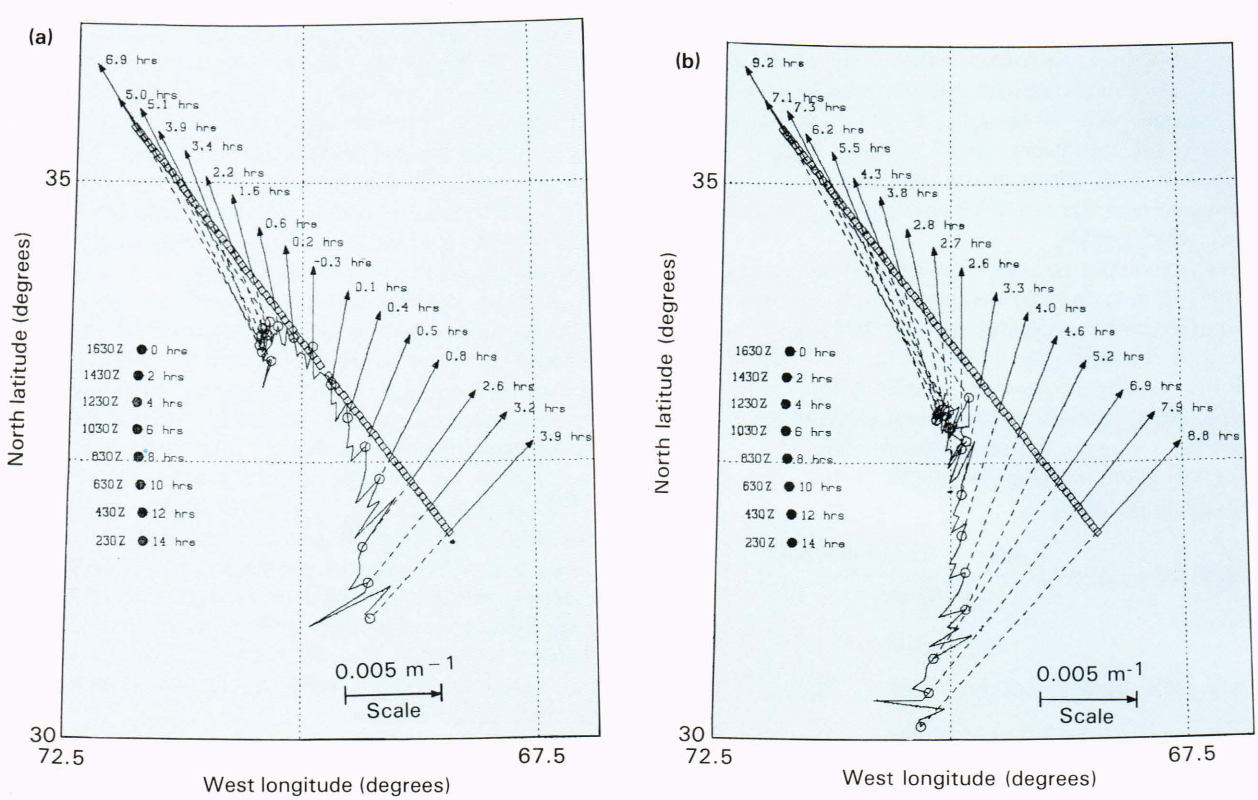

Figure 4—Hurricane best track, wavenumber vectors, and estimates of wave age and generation regions. Wave ages are given at the head of each wavenumber vector, and generating regions are indicated by open circles and the lines connecting them. Each figure represents solutions of Eqs. 2a-f for a different value of β in Fig. 3. (a) For $\beta = 0$ degrees. (b) For $\beta = 20$ degrees.

of storm movement. In contrast, the older waves at the northern end, although originating at a similar radius, appear to have been generated at a smaller azimuth of 60 to 80 degrees, while the southernmost waves were evidently generated at a much greater radius of 300 kilometers and an azimuth of 140 to 160 degrees.

A similar fan-shaped distribution of wave directions was observed during the Seasat mission in Hurricane Iva;[15] this characteristic pattern can be explained as a consequence of the circular geometry of the hurricane. However, the present analysis indicates that the waves observed in Josephine were generated at radii on the order of 200 to 300 kilometers, much greater than the radius of maximum winds (50 to 100 kilometers) that would be expected of a storm of Josephine's intensity. Thus, the particular dominant waves observed in such snapshots of hurricane wave fields are just a consequence of kinematics and the specific hurricane/image geometry and timing.

SUMMARY AND CONCLUSIONS

A simple kinematic model has been used in an analysis of one dominant wave system observed by SIR-B in Hurricane Josephine. The results suggest that waves were generated 0 to 9 hours before the SIR-B overpass, primarily in the right quadrant of the storm, at radii of several hundred kilometers.

REFERENCES

[1]V. F. Dvorak, "Tropical Cyclone Intensity Analysis and Forecasting from Satellite Imagery," *Monthly Weather Rev.* **103**, 420-430 (1975).
[2]R. C. Gentry, E. Rodgers, J. Steranka, and W. E. Shenk, "Predicting Tropical Cyclone Intensity Using Satellite-Measured Equivalent Blackbody Temperatures of Cloud Tops," *Monthly Weather Rev.* **108**, 445-455 (1980).
[3]L. A. Hughes, "On the Low-Level Wind Structure of Tropical Storms," *J. Meteor.* **9**, 422-428 (1952).
[4]W. M. Frank, "A Composite Analysis of the Core of a Mature Hurricane," *Monthly Weather Rev.* **112**, 2401-2420 (1984).
[5]D. P. Jorgensen, "Mesoscale and Convective-Scale Characteristics of Mature Hurricanes. Part II: Inner Core Structure of Hurricane Allen (1980)," *J. Atmos. Sciences* **41**, 1287-1311 (1984).
[6]I. M. Cline, "Relation of Changes of Storm Tides on the Coast of the Gulf of Mexico to the Center and Movement of Hurricanes," *Monthly Weather Rev.* **48**, 127-146 (1920).
[7]I. R. Tannehill, "Sea Swells in Relation to Movement and Intensity of Tropical Storms," *Monthly Weather Rev.* **64**, 231-238 (1936).
[8]G. Z. Forristall, E. G. Ward, V. J. Cardone, and L. E. Borgmann, "The Directional Spectra and Kinematics of Surface Gravity Waves in Tropical Storm Delia," *J. Phys. Ocean.* **8**, 888-909 (1978).
[9]E. G. Ward, L. E. Borgmann, and V. J. Cardone, "Statistics of Hurricane Waves in the Gulf of Mexico," *J. Petrol. Technol.* **31**, 632-642 (1979).
[10]Y. K. Lee, "Hurricane Eloise Wave Spectra," *Coastal Eng.* **4**, 151-156 (1980).
[11]K. E. Steele, J. C. Lau, and Y. L. Hsu, "Theory and Application of Calibration Techniques for an NDBC Directional Wave Measurements Buoy," *IEEE Trans. J. Oceanic Eng.* **OE-10**, 382-396 (1985).
[12]C. Elachi, T. W. Thompson, and D. King, "Ocean Wave Patterns Under Hurricane Gloria: Observation with an Airborne Synthetic-Aperture Radar," *Science* **198**, 609-610 (1977).
[13]D. B. King and O. H. Shemdin, "Radar Observations of Hurricane Wave Directions," in *Proc. 16th International Conf. Coastal Engineering,* Hamburg, Germany (1978).
[14]E. J. Walsh, D. W. Hancock III, and D. E. Hines, "Directional Wave Spectra Measured with the Surface Contour Radar," *J. Phys. Ocean.* **15**, 566-591 (1985).
[15]F. I. Gonzalez, T. W. Thompson, W. E. Brown, Jr., and D. E. Weissman, "Seasat Wind and Wave Observations of Northeast Pacific Hurricane Iva, August 13, 1978," *J. Geophys. Res.* **87**, 3431-3438 (1982).
[16]W. M. McLeish and D. B. Ross, "Imaging Radar Observations of Directional Properties of Ocean Waves," *J. Geophys. Res.* **88**, 4407-4419 (1983).
[17]R. C. Beal, F. M. Monaldo, D. G. Tilley, D. E. Irvine, E. J. Walsh, F. C. Jackson, D. W. Hancock III, D. E. Hines, R. N. Swift, F. I. Gonzalez, D. R. Lyzenga, and L. F. Zambresky, "A Comparison of SIR-B Directional Ocean Wave Spectra with Aircraft Scanning Radar Spectra," *Science* **232**, 1531-1535 (1986).
[18]G. B. Clark and M. B. Lawrence, "North Atlantic Tropical Cyclones," *Mar. Weather Log* **29**, 1-7 (1985).
[19]B. Holt and F. I. Gonzalez, "SIR-B Observations of Dominant Ocean Waves Near Hurricane Josephine," *J. Geophys. Res.* **91**, 8595-8598 (1986).
[20]G. C. Clark and R. A. Case, "Annual Data and Verification Tabulation Atlantic Tropical Cyclones 1984," NOAA Technical Memorandum NWS NHC 26 (1985).
[21]J. C. Curlander, "Performance of the SIR-B Digital Image Processing Subsystem," *IEEE Trans. Geosci. Remote Sens.* **GE-14**, 649-652 (1986).

ACKNOWLEDGMENT – We thank the Jet Propulsion Laboratory for the timely provision of the SIR-B imagery.